EXTENSION OF THE LIMITS OF THE XDH STRUCTURAL ELEMENT IN *DROSOPHILA MELANOGASTER*[1]

WILLIAM GELBART[2], MARGARET McCARRON AND ARTHUR CHOVNICK

Genetics and Cell Biology Section, Biological Sciences Group
University of Connecticut, Storrs, Connecticut 06268

Manuscript received April 29, 1976

ABSTRACT

Experiments expanding the array of mutants affecting the xanthine dehydrogenase (XDH) structural element in *Drosophila melanogaster* are described. These include rosy eye color mutants which exhibit interallelic complementation, and mutants with normal eye color but lowered levels of XDH. Evidence is presented which argues that these are structural alterations in the enzyme. Recombination experiments were performed using these mutants as well as some electrophoretic variants. The two ends of the rosy locus are marked with mutant sites which are clearly structural in nature; the XDH structural element and the rosy null mutant map are completely concordant. A possible procedure to recover control element mutants is described.

IT seems that much of the DNA in *Drosophila melanogaster*, as well as other higher eukaryotes, does not function as polypeptide-coding information. Results of physical studies of the Drosophila genome (LAIRD 1973; MANNING, SCHMID and DAVIDSON 1975) and of its transcriptional products (LEVY and McCARTY 1975) are consistent with this notion, as are the results of purely genetic analyses (JUDD, SHEN and KAUFMAN 1972; HOCHMAN 1973; LEFEVRE 1973). Such studies indicate that the number of mRNA species is equivalent to the number of genetic units, defined by complementation tests, and also to the number of polytene chromosome bands, or chromomeres. However, the amount of single copy DNA is an order of magnitude greater than the amount coding for identifiable polysomal mRNA. In addition, stretches of middle repetitive sequences appear to be interspersed among this single copy DNA. Considerable interest has been focused on the functions of the nonpolypeptide coding DNA (nonstructural DNA). Conceivably, at least some of this DNA contains control information for adjacent structural sequences. It is hoped that the elucidation of these control mechanisms will provide important insights into processes governing differential gene activity during development.

Obviously, one route to understanding these control mechanisms is through an examination of mutants affecting these processes. However, considering the enormous genetic variation observed in higher organisms, there is a striking

[1] This investigation was supported by research grant GM-09886 from the Public Health Service, and by research grant BMS74-19628 from the National Science Foundation.

[2] Present address: Department of Biology, Harvard University, Cambridge, Massachusetts 02138.

paucity of documented control variants. Quite possibly the source of this paucity is technical, i.e., in most interesting genetic systems, the necessary biochemical probes are lacking. The study of specific genetic systems controlling known biochemical reactions surmounts this difficulty.

We have been exploiting a favorable system of this sort, the rosy locus in *Drosophila melanogaster*, which is responsible for synthesis of the polypeptide subunit of xanthine dehydrogenase (XDH). The most attractive features of this system are that it possesses an easily recognizable mutant phenotype, that it is known to code for a particular enzyme (XDH), and that, due to chemical selection procedures, it is particularly amenable to fine structure recombination analysis (see MATERIALS AND METHODS). Making use of these features, we have undertaken an intensive analysis of the organization of this locus. Our strategy has been to identify the XDH-structural element within the rosy locus and then, using mutants which mark the borders of this structural element, distinguish those variants which modulate the synthesis of XDH, and which are not within the structural element (i.e., control element variants).

An initial description of the XDH-structural element was presented by GELBART *et al.* (1974). Unambiguous structural element sites—controlling electrophoretic mobility variations—were localized on a reference map of null-XDH sites, previously elaborated by CHOVNICK *et al.* (1964) and CHOVNICK, BALLANTYNE and HOLM (1971). The electrophoretic sites fell into two clusters, one near each end of the null mutant map. Utilizing a straightforward *cis-trans* test, we demonstrated that the entire region spanning these clusters codes for a single continuous polypeptide chain; this polypeptide is the subunit of the active XDH homodimer, identified by CANDIDO, BAILLIE and CHOVNICK (1974). Hence, we found that the XDH-structural element roughly corresponded to the map of null-XDH mutants.

We are most interested in identifying control element variants. One screen for such variants requires that they map beyond the boundaries of the XDH structural element. Since amino acid sequence data on XDH are not available, we must rely upon boundaries defined solely by genetic means. The present report is an intensive study of the XDH structural element, particularly focusing on its proximal (left hand) boundary. Our interest in this end is based upon the identification of a putative control element proximal to the structural element (CHOVNICK *et al.* 1976).

This paper deals with three classes of structural variants. We further localize three previously identified electrophoretic sites. In addition, we describe the properties of two new classes of rosy structural mutants: mutants exhibiting interallelic complementation and mutants with lowered levels of XDH. From these studies, we conclude that the entire array of rosy null-XDH mutants are defects in the XDH structural element.

MATERIALS AND METHODS

Background information: The rosy (*ry*) locus in *Drosophila melanogaster* is a genetic unit situated at position 52.0 on chromosome 3, and is defined by a set of recessive brownish eye color mutants. These allelic mutants are all defective in drosopterin pigments and all lack xanthine

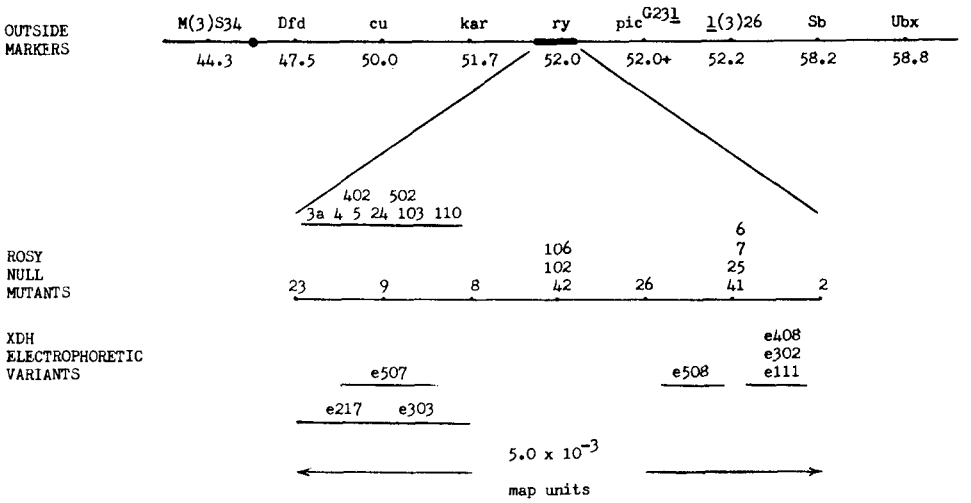

FIGURE 1.—The centromere-proximal region of chromosome *3*. Designations and map positions of mutants used in this study are presented. The expanded map represents rosy alleles which have been mapped to sites within the rosy locus. Both null mutant and electrophoretic variant sites are included.

dehydrogenase (XDH) activity. Intensive fine structure analysis of rosy mutants has led to the identification of several null mutant sites within the locus (CHOVNICK, BALLANTYNE and HOLM 1971). Figure 1 is a map of the centromere-proximal region of chromosome *3*, indicating the location of rosy, the centromere and other markers used in the present study (LINDSLEY and GRELL 1968). It also contains an expanded map of the known separable sites within the rosy locus. Note that the total map length of the rosy locus is listed as 5.0×10^{-3} map units, a far more reliable estimate, based on much larger samplings than the previous reported distance of 9.0×10^{-3} (CHOVNICK *et al.* 1964). Electrophoretic variants of XDH are controlled by genetic determinants mapping to the immediate vicinity of the rosy locus (YEN and GLASSMAN 1965). Recently, these determinants have been localized to sites within the rosy locus itself (GELBART *et al.* 1974). The positions of these sites are also summarized in Figure 1.

TABLE 1

The nomenclature for several ry+ *isoalleles*

	XDH electrophoretic mobility	
ry+ isoallele	Old designation	Revised designation
+*12*	none	0.90
+*13*	none	0.90
+*14*	none	0.94
+*10*	I	0.97
+ *0*	II	1.00
+ *6*	II	1.00
+ *1*	III	1.02
+ *4*	III	1.02
+*11*	III	1.02
+ *2*	IV	1.03
+ *3*	V	1.05
+ *5*	V	1.05

Nomenclature: Since our last report, we have found greater diversity than had been noted previously among our XDH electrophoretic variants. Our published nomenclature will not easily accommodate these new variants and so we are forced to change to a more elastic system. Table 1 presents the designations of our various isoalleles in both systems. The revised nomenclature simply describes any mobility relative to that of our standard isoallele, $ry+^{0}$. $ry+^{0}$ is designated as having a mobility of $XDH^{1.00}$. Relative mobility of isoallele $ry+^{x}$ = [distance migrated by isozyme $ry+^{x}$/distance migrated by the $ry+^{0}$ isozyme].

As before, isoalleles of ry+ are given numerical superscript designations (e.g., $ry+^{12}$). Null mutants are identified by a numerical superscript immediately following a *ry* prefix (e.g., ry^{103}, ry^{1201}) while electrophoretic mobility sites utilize a ry^{e} prefix (e.g., ry^{e217}). The isoallelic source of any rosy null mutant can be deduced from the first number(s) of the mutant designation—ry^{103} is derived from $ry+^{1}$, ry^{1201} from $ry+^{12}$ and ry^{5} from $ry+^{0}$ (ry^{5} is an abbreviation for ry^{005}).

Selective system matings: The experiments involved assaying *ry*+recombinants occurring in the meiocytes of heteroallelic rosy females of the type *kar* ry^{x} *l*/ry^{y}, ry^{x} being a mutant induced in one *ry*+ isoallele and ry^{y} being induced in a different isoallele. Either *l(3)26* or pic^{G23l} was used as the distal flanking marker (*l*). These females were mated to tester rosy males as indicated in Figure 2. Progeny were reared on medium supplemented with levels of purine known to be toxic to all individuals lacking XDH activity. Only rare *ry*+ recombinant progeny survived to adulthood. The protocol for conducting large scale crosses was the same as previously described (CHOVNICK 1973). Unless otherwise noted, all mutants and rearrangements are listed in LINDSLEY and GRELL (1968) or GELBART *et al.* (1974).

Tests of exceptional progeny: Surviving individuals of the selective system crosses could immediately be classified for karmoisin and rosy phenotypes. These survivors were crossed individually to *kar*^{2} *Df(3R)*ry^{75}*/ Tp(3)MKRS, M(3)S34 kar* ry^{2} *Sb* mates. The progeny phenotypes confirm the diagnoses with regard to karmoisin and rosy. The progeny were further tested in two ways: (1) testing for the allelic state of pic^{G23l} or *l(3)26* flanking marker by examining the progeny of males bearing the *ry*+ exceptional chromosome mated to females of an appropriate lethal-bearing stock, and (2) determining the mobility of the XDH produced by flies carrying the *ry*+ exceptional chromosome exposed by a deficiency of the rosy locus (either *Df(3R)*ry^{36} or *kar*^{2} *Df(3R)*ry^{75} was used). The procedures used in the XDH electrophoretic analysis are described by MCCARRON, GELBART and CHOVNICK (1974).

Mutagenesis procedures: A number of new rosy mutants described in this report were induced with EMS, according to the method of LEWIS and BACHER (1968). A 0.018 M solution of EMS was used. Other mutants were selected from among the progeny of males treated with 4500 rad. from a ^{137}Cs source. Only irradiated mature sperm from these males were sampled.

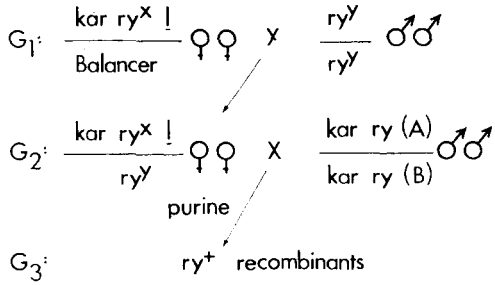

FIGURE 2.—The general protocol for intragenic recombination analysis at the rosy locus. The mutants ry^{x} and ry^{y} represent any two rosy heteroalleles. Either *l(3)26* or pic^{G23l} was used as the distal flanking marker. The G_2 males were always *kar ry* in phenotype. Either *Dfd Df(3R)*kar^{3l} ry^{60}*/*kar^{2} *Df(3R)*ry^{75} or *In(3L)P* + *In(3R)P18, Ubx* ry^{41} kar^{2} e^{4}*/Tp(3)MKRS, M(3)S34* kar^{4} ry^{2} *Sb (P18/MKRS)* males were used in crosses involving the mutant pic^{G23l}, which is lethal in combination with *Df(3R)*ry^{75}.

Purine sensitivity tests: The purine sensitivities of several induced mutants were determined and compared to the wild-type sensitivities. Males which were either *mutant/MKRS* or +/+ were mated to homozygous ry^{41} females, eliminating the possibility of maternal effect differences. Fifteen pairs of parents were placed in each bottle, and transferred every two days for a total of four broods. After the parents were removed from a culture, 1.0 ml. of purine was applied to the surface of the medium. Eight concentrations of purine were used: 0.2, 0.3, 0.4, 0.5, 0.6, 0.7, 0.8, and 1.0% purine (W/V). Six cultures were tested at each dose. Seventeen days after a culture was initiated, the number of (1) empty pupal cases, and (2) total number of pupae, on the walls of the culture vessel were counted. These counts were compared to their equivalents in untreated control bottles raised under identical conditions. For the mutants, control counts were halved to compensate for ry^{41}*/MKRS* offspring which die at every treatment dose. From these comparisons, % eclosion and pupation estimates were calculated for each dosage.

Fluorometric assay of XDH: The methods used are identical to those of CHOVNICK *et al.* (1970).

Rocket electrophoresis: The techniques used for rocket electrophoresis are described in CHOVNICK *et al.* (1976).

EXPERIMENTS AND RESULTS

In several of the data tables in this report (Tables 2, 3, 6, 7, 9, and 11) the results of fine structure recombination experiments are described. The experiments were designed such that only rare ry^+ recombinant progeny survived. In these tables, the ry^+ exceptional offspring are divided into four groups. The two crossover classes include the ry^+ exceptions which carry nonparental combinations of outside markers. Conversion classes form the other two groups. The rosy mutant which has been converted to ry^+ is identified by the set of parental outside markers that it carries. Within each group, the number of recovered ry^+ exceptions with a particular XDH electrophoretic mobility is provided. The mobility designations are presented in brackets.

In this report, we are concerned with the identification of the limits of the XDH structural element. An analysis of the data as it pertains to the mechanisms of recombination will not be undertaken here.

I. Further studies of electrophoretic variants:

In a previous report, the genetic bases of electrophoretic differences between ry^{+0} and ry^{+2}, and between ry^{+0} and ry^{+5}, were mapped to sites within the rosy locus (GELBART *et al.* 1974). Only one demonstrable electrophoretic difference (*e217*) was noted between the ry^{+0} [$XDH^{1.00}$] and ry^{+2} [$XDH^{1.03}$] isoalleles. The ry^{+0} isoallele possesses the slower allele at this site (*e217S*) while ry^{+2} carries the faster allele (*e217F*). The mobility difference that distinguishes ry^{+0} from ry^{+5} [$XDH^{1.05}$] was separated into two components: *e507* and *e508*; ry^{+0} carries the slow allele of both these sites (*e507S–e508S*) while ry^{+5} possesses both fast alleles (*e507F–e508F*). Recombinants which are *e507F–e508S* produce $XDH^{1.03}$ molecules while *e507S–e508F* individuals show a characteristic $XDH^{1.02}$ mobility. The sites *e217* and *e507* map near the proximal (left) end, and *e508* near the distal (right) end of the rosy null mutant map.

A number of fine-structure mapping experiments were carried out to refine the positions of these electrophoretic sites. We will first present our findings relative to the proximal sites *e217* and *e507*, and then relative to the distal *e508*

site. In addition to simply determining the order of the mutants, these crosses were constructed so that information on the locations of XDH electrophoretic site differences also could be culled. The key feature of the genetic system which enabled us to obtain this information is that the mutants were each induced in strains isogenic for a specific ry^+ isoallele of known XDH electrophoretic mobility. To illustrate the logic for mapping electrophoretic sites, let us review one cross in detail—the cross involving *kar* ry^{41} *l(3)26*/ry^{502} females (GELBART *et al.* 1974, reprinted in Table 2). The mutant ry^{41} was derived from ry^{+0} [$XDH^{1.00}$] while ry^{502} was derived from ry^{+5} [$XDH^{1.05}$]. Among a sample of 1.48×10^6 zygotes, 40 ry^+ exceptions were recovered. With respect to flanking markers, the exceptions were divided into three groups: 24 crossovers which were *kar* ry^+, 7 ry^+ exceptions which were conversions of ry^{502}, and 9 *kar* ry^+ *l(3)26* exceptions which were conversions of ry^{41}. The 24 crossovers serve to place ry^{502} proximal to (= to the left of) ry^{41}. All 40 ry^+ exceptions were characterized for electrophoretic mobility. If only one site of XDH electrophoretic difference distinguished ry^{+0} and ry^{+5}, then all ry^+ exceptions should be either $XDH^{1.00}$ or $XDH^{1.05}$. (Note that since only ry^+ recombinants are recovered, any alterations in electrophoretic mobility produced by the mutants ry^{41} and ry^{502} are eliminated as a consequence of the recombination event.) However, a novel and intermediate XDH-type was recovered ($XDH^{1.02}$). Therefore, there must be at least two

TABLE 2

Mapping e507 *and* e508

Crosses are of the type: *kar* ry^x *l(3)26*/ry^{500} ♀ ♀ × tester ry ♂ ♂

Parental alleles		Genotypes of ry^+ exceptional chromosomes				
		Crossovers		Conv. ry^{500}	Conv. ry^x	Sample
ry^x	ry^{500}	*kar* ry^+	ry^+ *l(3)26*	ry^+	*kar* ry^+ *l(3)26*	($\times 10^{-6}$)
*41**	*501*	0	0	0	0	1.37
26	*501*	0	0	0	2[1.00]†	0.82
8	*501*	0	9[1.03]	1[1.03]	12[1.00]	2.65
					[1.03]	
*5**	*501*	0	2[1.00]	2[1.03]	3[1.00]	0.84
			13[1.03]	2[1.05]	3[1.03]	
*41**	*502*	1[1.00]	0	6[1.02]	9[1.00]	1.48
		23[1.02]		1[1.05]		
26	*502*	28[1.02]	0	11[1.02]	12[1.00]	1.12
		2[1.05]		1[1.05]		
42	*502*	9[1.02]	0	14[1.02]	5[1.00]	1.54
				4[1.05]		
8	*502*	6[1.02]	0	8[1.02]	3[1.00]	1.83
				1[1.05]		
5	*502*	0	6[1.00]	12[1.02]	6[1.00]	2.20
			1[1.03]	4[1.05]		
*5**	*506*	0	3[1.03]	0	4[1.00]	0.90

* Data taken from GELBART *et al.* (1974).

† [1.00] = *e507S e508S*; [1.02] = *e507S e508F*; [1.03] = *e507F e508S*; [1.05] = *e507F e508F*.

mobility differences between ry^{+0} and ry^{+5}. We can rewrite the 41/502 females as: $\frac{kar \; + \; e507S \; e508S \; 41 \; l(3)26}{+ \; 502 \; e507F \; e508F \; + \; +}$ · Twenty-three of the *kar* ry^+ crossovers were $XDH^{1.02}$; these were crossovers between *e507* and *e508* and were genotypically *kar e507S e508F*. The other crossover, *kar* ry^+, $XDH^{1.00}$ occurred between *e508F* and *41*, and was *kar e507S e508S*. Hence, *e508* must be fairly close to *41*, since only one of 24 crossovers separated them. No co-conversions of *41* and *e508* occurred. None of the crossovers separated *502* and *e507*, therefore, their relative order is not known. However, these two sites must be very close, since only one conversion of ry^{502} to ry^+ [$XDH^{1.05}$] was not a co-conversion of *e507F* to *e507S*, while the other 6 conversions were $XDH^{1.02}$ and therefore co-conversions of *e507F* to *e507S* (see footnote to Table 2). Thus, these data are consistent with two XDH electrophoretic sites differences between ry^{+0} and ry^{+5}: one proximal, but very near ry^{41} (*e508*) and the other very close to ry^{502} (*e507*). As will be described below, the logic used to analyze this cross can be extended to any of the crosses in this manuscript, and provide us with a coherent picture of the locations of the electrophoretic sites described herein.

A. *Mapping* e507 *and* e217:

Let us first discuss the position of *e507*. Table 2 presents the results of a series of crosses testing *501*, *502*, and *506* against the reference alleles *5*, *8*, *42*, *26*, and *41*. On the basis of crossover data, *501* is located in the vicinity of *26* and *41*. The mutant *502* falls approximately midway between 5 and *8*. Judging from the direction and frequency of crossovers between 5 and *506*, *506* probably lies in the vicinity of *8* or *42*.

The electrophoretic site *e507* is approximately equidistant from *5* and *8*. A total of eight crossovers in 3.04×10^6 progeny place *e507* distal to *5* (see the *5/501* and *5/502* crosses, Table 2), while six crossovers in 1.83×10^6 progeny place *e507* proximal to *8* (see the *8/502* cross, Table 2). The position of *502* relative to *e507* is unclear. The progeny of *26/502* females included two *kar* $XDH^{1.05}$ crossovers, indicating that *e507* is distal to *502*. In contradistinction, the one $XDH^{1.03}$ *l(3)26* crossover generated by *5/502* females puts *e507* proximal to *502*. We know that *e507* and *502* are very close to each other, since they exhibit a very high rate of co-conversion. Among 62 conversions of *502* in Table 2, 51 are co-conversions of *e507* ($XDH^{1.03}$). This is a much higher co-conversion rate than that of *e507* with either *5* or *8* (3/10 and 1/10, respectively). Hence, we conclude that *e507* is located very near *502*, approximately midway between *5* and *8*; the relative order of *e507* and *502* cannot be ascertained. In this case we may have encountered a real lower limit to recombination analysis.

Turn to the localization of *e217*. Data pertaining to this electrophoretic site are summarized in Table 3. Crosses of *41* to four *200* series mutants served to place *e217* proximal to, and distant from, *41* (GELBART *et al.* 1974). Several other crosses were carried out to further resolve its map position. Crosses of *8* to *203* and *207* place these *200* alleles distal to *8* and place *e217* in the interval from the proximal end of the structural element to just distal to *8*. (Experiments which

TABLE 3

Mapping e217

Crosses are of the type: *kar* ry^{x} *l(3)26*/ry^{200} ♀ ♀ × tester *ry* ♂ ♂

ry^{x}	ry^{200}	Crossovers		Conv. ry^{200}	Conv. ry^{x}	Sample ($\times 10^{-6}$)
		kar ry+	*ry*+ *l(3)26*	*ry*+	*kar ry*+ *l(3)26*	
*41**	*201*	8[1.00]†	0	3[1.00]	10[1.00]	0.74
*41**	*203*	0	0	1[1.03]	1[1.00]	0.69
*41**	*204*	6[1.00]	0	7[1.00]	6[1.00]	0.68
				1[1.03]		
*41**	*205*	4[1.00]	0	6[1.03]	5[1.00]	0.66
8	*203*	0	3[1.03]	16[1.03]	3[1.00]	1.07
					1[1.03]	
8	*207*	0	6[1.03]	2[1.03]	2[1.00]	0.75
					3[1.03]	
5	*203*	0	2[1.00]	6[1.03]	3[1.00]	1.50
			17[1.03]		3[1.03]	

* Data taken from GELBART *et al.* (1974).
† [1.00] = *e217S*; [1.03] = *e217F*.

will be presented in a later section demonstrate that *e217* is proximal to *8* [see line 1 in Table 9].) Two of the crossovers recovered from the 1.5×10^{6} progeny of *5/203* females position *e217* distal to *5*. Note that the co-conversion properties of *e217* are similar to those of *e507*. While *e217* co-converts with both *5* and *8* at moderate frequencies, it co-converts at much higher rates with *201* and *204*. We infer that both *201* and *204* also lie between *5* and *8*, but confirming experiments have not been undertaken.

B. *Mapping* e508:

From Table 2, we can extract data which indicates that *e508* falls between *26* and *41*. One crossover in 1.48×10^{6} progeny of *41/502* females separated *e508* from *41*, placing the former proximal to the latter. In the cross of *26/502*, none of the thirty crossovers separated *e508* from *26*. This suggests that *e508* resides somewhere in the interval extending from just proximal to *26* to just proximal to *41*. This is consistent with the conversion data. We have not observed co-conversion of *e508* with either *26* or *41*, but *e508* does co-convert with *501*. Moreover, *501* has not been separated from either *26* or *41*. Tentatively, these data conspire to place *e508* and *501* between *26* and *41*.

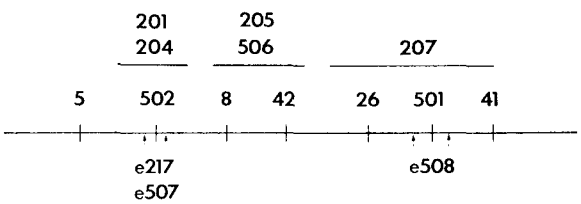

FIGURE 3.—A summary map of experiments localizing *e217*, *e507* and *e508*.

Figure 3 summarizes these results concerning the positions of null alleles and electrophoretic sites in the +0, +2 and +5 series.

II. Identification and localization of complementing mutants:

A. *Identification*:

Early work on the rosy locus did not uncover any examples of interallelic complementation, and led to the description of the rosy locus as a simple cistron (SCHALET, KERNAGHAN and CHOVNICK 1964). However, interallelic complementation is often noted among structural mutants in loci contributing to multimeric enzymes. Since we recently demonstrated that XDH is a homodimer coded by the rosy locus (GELBART *et al.* 1974), we reopened the possibility of complementation between rosy mutants. Complementing mutants would provide us with another probe of the structural element. In addition to the array of X-ray induced and spontaneous mutants available to SCHALET, KERNAGHAN and CHOVNICK (*loc. cit.*), we had available additional radiation-induced mutants and a series of EMS-induced alleles. The rosy phenotype is a very sensitive indicator of XDH activity. Genotypes conferring the mutant eye color have no detectable XDH activity and conversely, a modicum of XDH produces wild-type eye color. Homozygotes for any of the known rosy alleles exhibit the mutant eye color. To detect complementation, *trans* heterozygotes were constructed and their eye color phenotypes scored.

Twenty-four rosy eye color mutants were tested *inter se*. Twenty-one of these alleles were EMS-induced, two were spontaneous and one was radiation-induced. Cultures were reared at 25° and were allowed to accumulate adult offspring for three to four days before being screened for eye color. Of these twenty-four mutants, seven exhibited partial or full restoration of the normal eye color in one or more heterozygous combinations. These seven complementing mutants (six EMS-induced and one spontaneous) were then used as testers to screen an additional forty radiation-induced and three EMS-induced rosy alleles. This screen detected four more complementing mutants (three radiation and one EMS-induced). These four mutants were then tested in pairwise combinations. Hence, all complementing mutants were tested *inter se*.

In all, eleven rosy mutants displayed interallelic complementation. This screen for complementing mutants was not intended to be exhaustive. Most of the radiation-induced mutants have not been screened in all pairwise combinations. Moreover, the possibility of complementation was only assayed at a single temperature and with a single phenotype—the eye color. We assume that we are underestimating the number of complementing alleles among the available mutants.

Table 4 contains the results of the *inter se* complementation tests of the eleven complementing mutants. Note that only fifteen of the forty-five mutant pairs exhibit any phenotypic complementation. Figure 4 contains the complementation map generated from the data in Table 4. The map is circular and is separated into eight complementation groups. See the legend to Figure 4 for a cataloging of the mutants in each group. A nonlinear complementation map is indicative of inter-

TABLE 4

The interallelic complementation pattern of rosy mutants tested as ry^x/ry^y heterozygotes

	ry^x										
ry^y	*2*	*42*	*60*	*207*	*406*	*501*	*602*	*606*	*609*	*1003*	*L.19*
L.19	—	—	—	—	+	—	+	+	—	—	—
1003		—	—	—	+	—	—	—	—	—	
609	—	—	—	—	+	—	+/—	+	—		
606	—	+	+	+/—	—	+	—	—			
602	—	—	—	—	—	—	—				
501		—	—	—	+	—					
406	+/—	+	—	+	—						
207	—	—	—	—							
60		—	—								
42		—									
2	—										

Key: + = wild-type eye color
+/— = intermediate eye color
— = mutant eye color.

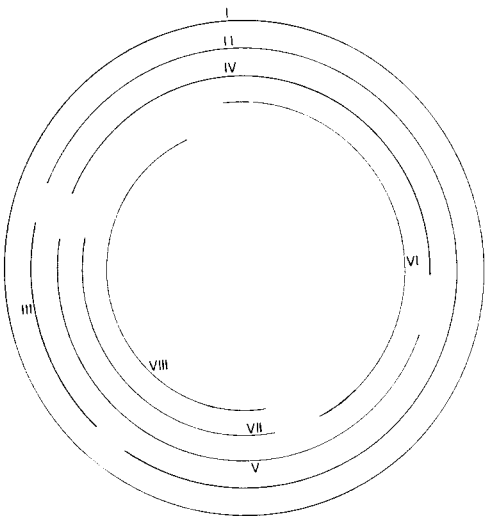

FIGURE 4.—The complementation map of the rosy locus. Mutants are divided into complementation groups I through VIII. Complementation groups whose lines do not overlap are complementary. The mutants in each group are as follows. I–56 mutants: *1, 3a, 4, 5, 6, 7, 9, 17, 18, 19, 20, 21, 23, 24, 26, 40, 41, 45, 48, 56, 57, 58, 59, 61, 62, 63, 64, 102, 103, 106, 110, 201, 203, 204, 205, 206, 208, 209, 210, 301, 404, 405, 502, 506, 601, 603, 604, 605, 607, 608, 1001, 1002, L.12, L.14, L 18.* II–1 mutant: *602.* III–2 mutants: *609, L.19.* IV–1 mutant: *606.* V–1 mutant: *60.* VI–1 mutant: *406.* VII–3 mutants: *42, 207, 501.* VIII–1 mutant: *1003.*

allelic complementation. The standard mechanism invoked to explain this sort of complementation involves restoration of activity in hybrid multimers composed of defective subunits from each of the complementing alleles (CRICK and ORGEL 1964; FINCHAM 1966). Quite often, this phenomenon generates only partial restoration of enzyme activity. This is certainly true of the complementing rosy mutants. Extracts of complementing rosy heterozygotes were assayed fluorometrically for XDH activity, and their activities were compared to the activity of matched extracts of a standard wildtype, *+6*. The results of these assays, shown in Table 5, are expressed as % of *+6/+6* XDH activity. If the complementing mutants produced hybrid dimers which were completely active, and if dimer formation were random, we would expect that the complementing mutants would exhibit roughly 50% of wild type XDH activity. Instead, however, we see a range of activities from < 1% to 16%. These activity levels should not be taken too literally. Since we might expect complementing XDH to be more labile than the wild type enzyme, the comparison of these activity levels to *in vivo* levels is suspect.

In support of the subunit interaction model of complementation, we can demonstrate a structural alteration in at least one complementing mutant. The complementing mutants *606* and *609* are derived from the same isoallele, *+6*. Extracts of *+6/+6* and *606/609* flies were analyzed for XDH mobility. The complementing heterozygote XDH migrated faster (1.02) then the wild-type enzyme (1.00). Therefore, one or both of the mutant alleles is altered in net charge relative to *+6*. The identification of a structural alteration is consistent with the aforementioned model of complementation.

TABLE 5

The XDH activity of complementing pairs of rosy mutants (expressed as % of +6/+6 activity)

Mutant pairs	Experiment 1	Experiment 2
L.19/406	16	6
609/406	9	–
207/406	8.5	–
L.19/602	7	–
L.19/606	5.5	–
609/606	2.5	–
207/606	1	–
609/602	–	2.3
1003/406	–	2.3
42/406	–	1.6
501/406	–	1.4
2/406	–	0.8
501/606	–	0.2
42/606	–	0.2

TABLE 6

Localizing the complementing rosy alleles relative to ry^8. *Crosses are of the type:* cu kar ry^8 l(3)26/ry^c ♀ ♀ × Dfd Df(3R)kar^{31} ry^{60}/kar^2 Df(3R)ry^{75} ♂ ♂

	Crossovers		Conv. ry^8	Conv. ry^c	
ry^c	*kar ry+*	*ry+ l(3)26*	*kar ry+ l(3)26*	*ry+*	Sample ($\times 10^{-6}$)
207	0	6[1.03]	2[1.00] 3[1.03]	2[1.03]	0.75
406	1[1.02]	0	2[1.00]	0	0.57
602	3[1.00]	0	1[1.00]	3[1.00]	0.77
606	3[1.00]	0	2[1.00]	2[1.00]	0.64
609	0	3[1.00]	5[1.00]	3[1.00]	0.69
L.19	0	3[0.90]	0	2[0.90] 1[0.94]	0.72

B. *Localization*:

The identification of interallelic complementation provided us with another class of structural mutants. Since they might extend the limits of the XDH structural element, we proceeded to map them.

Three complementing mutants had been used as standard null mutants and so were already localized (*2*, *42* and *501*). The mutant *501* falls between *26* and *41*, while *42* is between *8* and *26*; both are within the known structural element (GELBART *et al.* 1974). The position of *2* is distal to *41* (CHOVNICK, BALLANTYNE and HOLM 1971).

Since the complementing mutants are homozygous null alleles, they could be mapped directly by the purine selection procedure. Table 6 summarizes the results of the first set of crosses, in which *207*, *406*, *602*, *606*, *609* and *L.19* were tested against *cu kar* ry^8 *l(3)26*. We were particularly interested in dissecting the proximal end of the structural element. The crosses to *8* permitted rapid identification of proximal alleles. Those complementing mutants which produced *kar ry+* crossovers are proximal to *8* (*406*, *602* and *606*) while those which produced *ry+ l(3)26* crossovers are distal (*207*, *609* and *L.19*). The latter were not subjected to further tests. We have not carried out recombination experiments with *60* and *1003*.

We then concentrated on positioning the proximal complementing mutants. The results of the *inter se* crosses which established their positions are summarized in Table 7. Four *kar ry+* crossovers were recovered from among the

TABLE 7

Ordering the proximal group of complementing rosy alleles. Crosses are of the type: kar^2 ry^{406} pic^{G231}/ry^c ♀ ♀ × P18, Ubx ry^{41} kar e^4/kar^2 Df(3R)ry^{75} ♂ ♂

	Crossovers		Conv. *406*	Conv. ry^c	
ry^c	*kar ry+*	*ry+* pic^{G231}	*kar ry+* pic^{G231}	*ry+*	Sample ($\times 10^{-6}$)
606	4[1.00]	0	1[1.02]	6[1.00]	0.98
602	0	0	0	0	1.44

0.98×10^6 progeny of *kar*^{2} *ry*^{406} *pic*^{G231}/ *ry*^{606} females; these crossovers place *606* proximal to *406*. No *ry*$^+$ recombinants between *406* and *602* arose in a screen of 1.44×10^6 offspring. Obviously, these two mutants must be very near one another. Since they both must be distal to *606*, no further attempts to separate them were undertaken.

III. Mutants with reduced XDH levels:

A. *Identification*:

Conceivably, mutants with low levels of XDH can be identified in a variety of ways: through direct screening of enzyme activity, by scoring for intermediate eye color, or on the basis of increased sensitivity to enzyme inhibitors. We chose to select mutants via the last criterion, taking advantage of the increased purine sensitivity of larvae with reduced levels of XDH.

The mutagenesis scheme used to generate these mutants is diagrammed in Figure 5. Wild-type males (either *+2* or *+6*) were treated with EMS and mated to *ry Sb Ubx/ DCxF* females as shown in Figure 5, G_1. These males were allowed to mate for three hours after the cessation of treatment; hence, only postmeiotic stages were sampled. This protocol eliminates the possibility of recovering clustered mutational events.

The non-Dichaete G_2 individuals were scored for eye color. Rosy mutants were identified, and if fertile, put into balanced stocks. Individual *+*/ry Sb Ubx* males

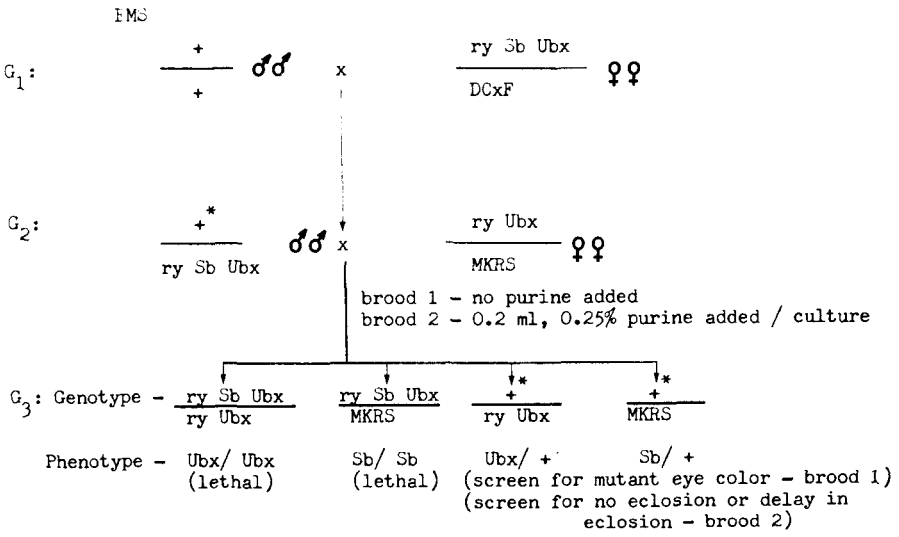

FIGURE 5.—The protocol for generating mutants hypersensitive to purine (*ry*^{ps}). G_1 males are mutagenized and mated *en masse* to G_1 females for three to four hours, and then discarded. The G_2 matings involved single males mated to three females per vial culture (brood 1). After four to five days, the parents are transferred to a fresh vial (brood 2). Three days later, the parents are discarded and purine is added to the brood 2 cultures.

TABLE 8

Results of screens for purine-sensitive rosy alleles utilizing the protocol outlined in Figure 6

Isoallele mutagenized	Chromosomes screened	Phenotype of recovered mutants	
		ry eye color (null-XDH)	*ry*$^+$ eye color (XDH$^+$)
+2	3382	9	11
+6	2101	4	4
Total	5483	13	15

(phenotypically *ry*$^+$) were crossed to three *ry Ubx/ MKRS* females per vial (brood 1). After four to five days, these parents were transferred to fresh vials (brood 2). Three days later, the parents were discarded and 0.2 ml of a 0.25% (W/V) aqueous purine solution was added to each brood 2 vial. Any G_3 zygotes receiving the *ry Sb Ubx* chromosome were inviable by virtue of being either *Sb/ Sb* or *Ubx/ Ubx*. The other two classes of progeny survived and were screened for purine sensitivity in brood 2 and for rosy eye color mutants in brood 1. Since the G_2 males were all *ry*$^+$ in phenotype, any G_3 rosy mutants arose from mosaic fathers.

Seven of the rosy mutants recovered in the G_3 possessed completely mutant germ lines while six have mosaic gonads. Brood 2 vials were screened every two to three days in the interval from nine to eighteen days after brood 2 was initiated. Without reliance on eye-color phenotype, this procedure allowed the recovery of mutants which are delayed in eclosion by purine, as well as the more extreme mutants which are unable to either pupate or eclose. Table 8 summarizes the results of these screens.

B. *Characterization:*

Obviously, purine sensitivity can be engendered by a number of routes. For the purposes of this report, we will only deal with three of the mutant strains recovered from these screens. These mutants, *ps214*, *ps611* and *ps612* (*ps* = purine sensitive), are all recessive to *ry*$^+$, exposed by deficiencies which delete the rosy locus, and allelic to rosy null mutants. They are also characterized by their wild-type eye color. XDH activity was assayed in these three strains, and also in their progenitor isoalleles. Extracts from adults homozygous for *ps611* and *ps612* exhibited 1% and 5% of the XDH activity of comparable *+6* extracts, respectively. Extracts of homozygous *ps214* imagoes had 24% of the XDH activity of matched *+2* extracts. Extracts from these five strains were also compared for the amount of antigen reacting with anti-XDH antisera, using the "rocket" electrophoresis of LAURELL (1966). When the immunoprecipitation reactions are run to completion, the heights of the peaks (or rockets) are proportional to the amount of XDH antigen in each sample. Due to the low activity of the purine-sensitive mutant extracts, the "mutant" rockets have been characterized by less intense staining of the XDH-precipitin line. These gels have not been suitable for photographic reproduction, and instead, we present a line drawing of a typical gel in Figure 6. Note that the heights of the mutant and wild-type peaks are essentially identical.

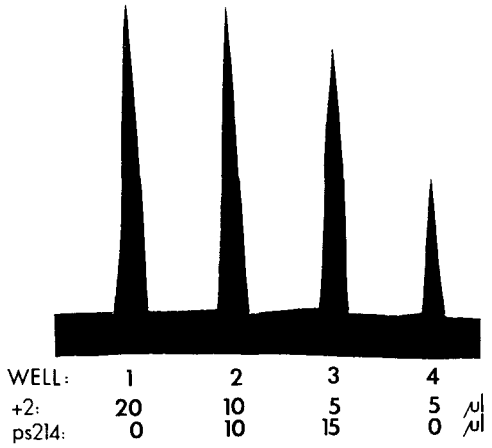

FIGURE 6.—Rocket electrophoresis analysis of *ps214 vs.* +*2*. This diagram depicts the heights of XDH peaks elicited by various mixtures of +*2* and *ps214* extracts reacting with anti-XDH antiserum. The XDH activity of *ps214* alone was too low to be visualized on these gels.

Therefore, the amounts of cross-reacting material present in these purine-sensitive mutants are essentially identical to their matched wild-type extracts. In other words, the specific activities of the mutant enzymes are much lower than normal, and hence, these mutants must be in the XDH structural element.

In order to ascertain if these mutants could be directly mapped, their purine sensitivities were measured (MATERIALS AND METHODS). The resulting purine sensitivity curves are presented in Figure 7. Indeed, the mutants are much more purine-sensitive than their wild-type counterparts. The differences in purine-

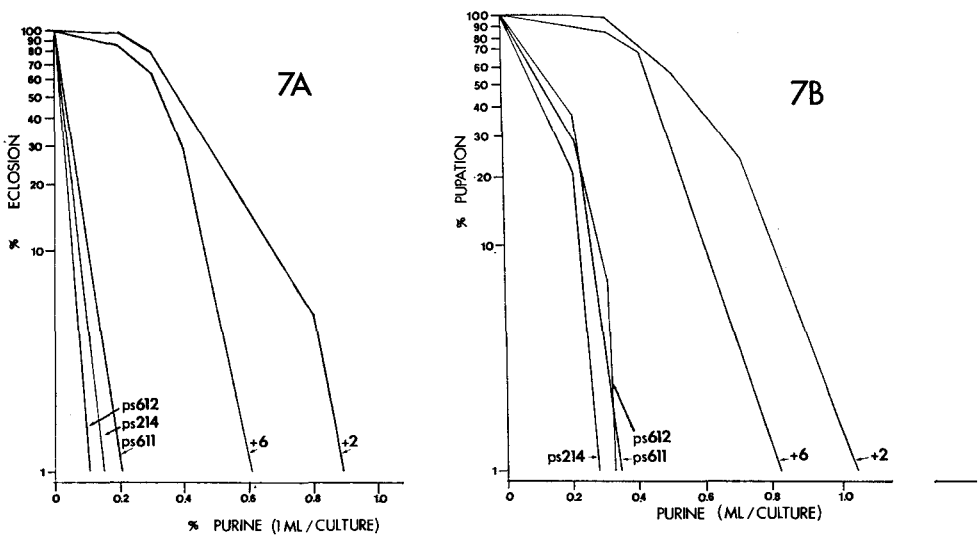

FIGURE 7.—The purine sensitivity of various mutant and wild-type rosy alleles. Figure 7A contains the relationship between frequency of eclosion and purine dosage for each genotype, while figure 7B relates this dosage to the frequency of pupation.

TABLE 9

Localizing the purine-sensitive rosy alleles relative to ry^8. *Crosses are of the type:* kar ry^8 l(3)26/ry^{ps} ♀ ♀ × *tester* ry ♂ ♂

ry^{ps}	Crossovers: *kar ry+*	Crossovers: *ry+ l(3)26*	Conv. ry^8: *kar ry+ l(3)26*	Conv. ry^{ps}: *ry+*	Sample ($\times 10^{-6}$)
ps214	1[1.00]	0	1[1.03]	1[1.00] 2[1.03]	0.74
ps611	0	3[1.00]	0	0	0.58
ps612	0	2[1.00]	2[1.00]	1[1.00]	0.60

sensitivity are more than sufficient to map the mutants via our standard selective protocol.

C. *Localization*:

We then proceeded to map these mutants in analogous fashion to the mapping of null-XDH mutants. The three purine-sensitive mutants were first tested with *cu kar* ry^8 *l(3)26*. The results of these crosses are in Table 9. The *ry+l(3)26* crossovers place *ps611* and *ps612* distal to *8*; these distal mutants were not tested further. On the basis of the one *kar ry+* crossover, *ps214* must be proximal to *8*. Note that this crossover has an $XDH^{1.00}$ mobility. It also serves to place *e217* proximal to *8* (See RESULTS, Section I). Further localization of *ps214* will be described in the following section.

IV. Establishing the order of the proximal structural mutants:

Where do the structural mutants lie relative to our standard null mutants and to each other? Specifically, what is the order of the most proximal sites from each class of structural variant: $e^2 17$, *e507*, *406*, *602*, *606* and *ps214*? Since these mutants are from a variety of isoallelic backgrounds, we should review the organization of electrophoretic mobilities of these isoalleles. This is done in Table 10. Essentially, *+0*, *+4 and +6* have identical proximal electrophoretic compositions which confer slower migration than the alternatives possessed by *+2* and +5.

To align these proximal structural variants, several recombination experiments were carried out. The results of these experiments are summarized in Table 11. These data provide unambiguous evidence that *606* is the most proximal structural variant thus far identified.

TABLE 10

The distribution of electrophoretic sites among five ry+ *isoalleles*

ry+ isoallele	Proximal sites: *e217*	Proximal sites: *e507*	Distal sites: *e408*	Distal sites: *e508*	Electrophoretic mobility
+0	S	S	S	S	1.00
+2	F	S	S	S	1.03
+4	S	S	F	S	1.02
+5	S	F	S	F	1.05
+6	S	S	S	S	1.00

TABLE 11

Ordering the proximal structural sites. Crosses are of the type: kar ry^x l*/ry^y ♀♀ ×*tester* ry ♂♂

ry^x chromosome	ry^y	Crossovers		Conv. ry^x	Conv. ry^y	Sample ($\times 10^{-6}$)
		kar ry+	*ry+ l**	*kar ry+ l**	*ry+*	
kar² 506 l(3)26	*ps214*	4[1.03]	0	0	6[1.03]	1.50
kar 41 l(3)26	*ps214*	15[1.00]	0	6[1.00]	1[1.00]	0.95
		7[1.03]		1[1.03]	6[1.03]	
kar² 406 pic^{G2sl}	*ps214*	1[1.03]	0	2[1.02]	1[1.03]	1.99
				1[1.05]		
kar² 606 l(3)26	*ps214*	0	7[1.00]	4[1.00]	1[1.00]	1.72
				1[1.03]	2[1.03]	
kar² 606 l(3)26	*502*	1[1.02]	5[1.00]	5[1.00]	5[1.02]	1.24
					1[1.05]	
cu kar 23 l(3)26	*406*†	0	2[1.00]	8[1.00]	2[1.02]†	1.21

* Either *l(3)26* or *pic^{G2sl}* was used as the distal flanking marker in any cross.
† This class may be underestimated because conversions of *406* carried *pic^{G2sl}* and were inviable with one of the two *ry* tester chromosomes (*kar² Df(3R)ry^{75}*) carried by their fathers.

First, consider the two electrophoretic sites, *e217* and *e507*. Both sites are located in the middle of the *5–8* interval. They produce identical shifts in electrophoretic mobility and could conceivably represent independent isolates of the same variant. To determine if they were separable, *ry^{ps214}/ kar² ry^{506} l(3)26* females were crossed to to tester *ry* males and their progeny reared on purine supplemented media (Table 11, Row 1). The electrophoretic sites are spanned, with *ps214* proximal (see below) and *506* distal. Ten *ry*+ offspring were recovered in 1.50×10^6 progeny. Four were *kar* ($XDH^{1.03}$) crossovers and six were conversions of *ps214* ($XDH^{1.03}$). Thus, all ten exceptions exhibited segregation of *e217* from *e507*. At present we have no evidence that the *e217* and *e507* sites are separable by recombination.

Now, turn to the localization of *ps214* relative to the *e217* site. The crossover recovered from *8/ ps214* females places both *e217* and *ps214* proximal to *8* (See RESULTS, Section III and Table 9). While *ps214* and *e217* are separable (since two of three conversions of *ps214* to + were not co-conversions of *e217*), this cross did not identify their relative order. To do so, *ps214* was crossed to the distal *+0* mutant, *41* (Table 11, Row 2). Twenty-two crossovers separating these two mutants were recovered in 0.95×10^6 zygotes. Seven of these crossovers were between *ps214* and *e217*, while the remainder were between *e217* and *41*. Therefore, *ps214* is proximal to *e217*.

Where does *406* lie relative to these sites? From *406/ ps214* females, one *kar ry*+ crossover was recovered among 1.99×10^6 progeny. This crossover, with a mobility of $XDH^{1.03}$, places *ps214* proximal to *406* and to *e217*. Since two of three conversions of *406* to + were co-conversions of *e217S* to *e217F*, *406* must be fairly close to this electrophoretic site. We should also note that *ps214* and *406* are much closer (one crossover in 1.99×10^6 progeny) than are *ps214* and *e217* (seven crossovers in 0.95×10^6 progeny). Recall that *406* was inseparable from another complementing mutant, *602*, in a sample of 1.44×10^6 zygotes (Table 7). There-

fore, we place *406* (and tentatively, *602* as well) between the structural sites *ps214* and *e217*.

Finally, turn to a consideration of the position of *606*. Previously, we had determined that *606* is proximal to *406* (Table 7). Since *406* is in turn proximal to *e217*, *606* will also be proximal to this electrophoretic site. We confirmed this expectation and at the same time positioned *606* relative to *ps214* (Table 11). Females of the genotype $kar^2\ ry^{606}\ l(3)26/\ ry^{ps214}$ gave rise to seven $ry^+\ l(3)26$ crossovers in 1.72×10^6 offspring; these crossovers indicate that *606* is proximal to *ps214*. Since they were $XDH^{1.00}$, these crossovers also place *606* proximal to *e217*, as expected. Interestingly, *e217* co-converted once with *606* and once with *ps214*. While we have independent evidence that *e217* and *e507* are fairly close, if not inseparable, we felt that we should directly position *e507* relative to *606*. This was accomplished by crossing $kar^2\ ry^{606}\ l(3)26/\ ry^{502}$ females to tester *ry* males. From among 1.24×10^6 zygotes, seventeen ry^+ exceptions were recovered (Table 11). Note that for the first time in all the rosy fine structure experiments, both types of crossovers (*kar* ry^+ and $ry^+\ l(3)26$) were recovered in one cross. Presuming that the majority crossover class is diagnostic for the true order of the mutants, we infer that *606* is proximal to both *502* and *e507* (based on the five $ry^+\ l(3)26$. $XDH^{1.00}$ crossovers). The minority class crossover, $kar^2\ ry^+$, $XDH^{1.02}$, is most easily visualized as a double event: a co-conversion of *502* and *e507* plus a crossover in the *kar* to *ry* interval. Assume this origin to be correct. Then, there are seven conversions of *502 to* +, of which six are associated with co-conversion of *e507F* to *e507S*. None of the five conversions of 606 were co-co-conversions of *e507*. Thus all data concerning *606* is consistent with its placement proximal to all other structural mutants.

The null-XDH mutant, *23*, appears to be the most proximal of the functionally undefined eye color mutants (CHOVNICK *et al.* 1964). We can indirectly estimate the position of *23* relative to *606* by comparing the frequency of *23/ 406* crossovers (Table 11) to *606/406* crossovers (Table 7). The former frequency was obtained by selecting for ry^+ recombinants in $cu\ kar\ ry^{23}\ l(3)26/\ ry^{406}\ pic^{G23l}$ females mated to $Dfd\ Df(3R)kar^{3l}\ ry^{60}/\ kar^2\ Df(3R)ry^{75}$ males. Two $ry^+\ l(3)26$ crossovers were recovered among 1.21×10^6 progeny, placing *23* proximal to *406*. A similar cross of *606* and *406* generated four crossovers among 0.98×10^6 progeny. The frequency of *23–406* crossovers is less than half that of *606–406* crossovers. While the samples are small, the data make it doubtful that *23* is in reality proximal to *606*. Indeed, STEPHEN CLARK in our laboratory has attempted to separate *606* and *23* and recovered no ry^+ survivors in a sample of 2.20×10^6 zygotes (personal communication). Hence, we must conclude that *606* and *23* occupy very close (if not identical) sites and represent the most proximal rosy mutants thus far mapped.

DISCUSSION

The XDH structural element revisited:

The data presented herein have described new probes of the XDH structural element and have refined and extended its boundaries. Figure 8 summarizes the

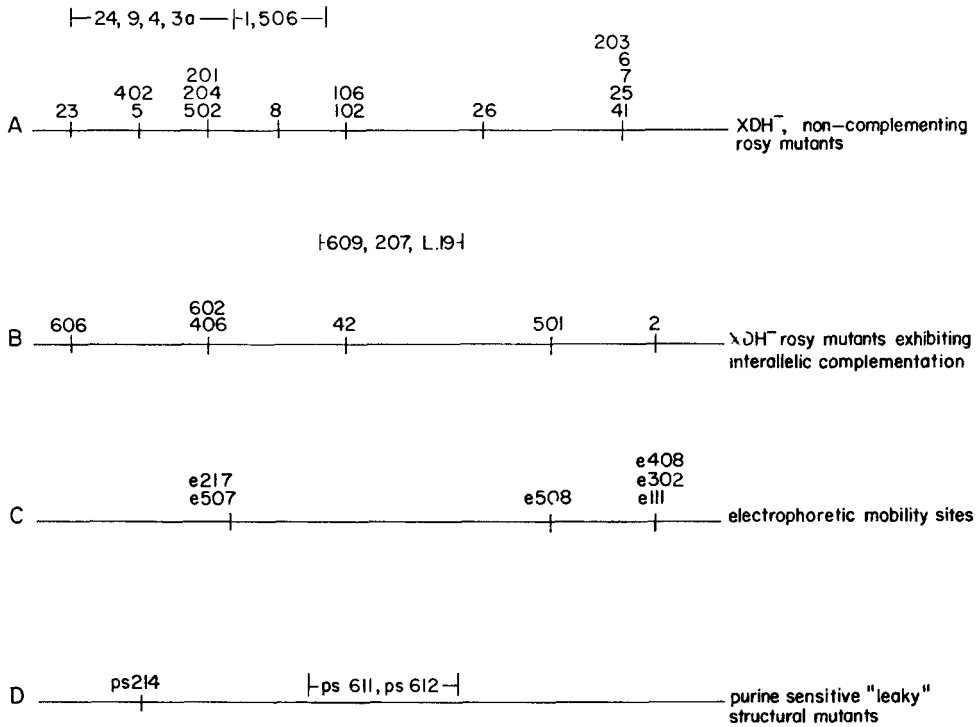

FIGURE 8.—Maps of the rosy locus, summarizing all recombination experiments involving rosy heteroalleles. The sites in these maps are aligned according to their positions relative to mutants in the other maps.

recombinational information generated in this study. We have identified a total of nine sites definitely associated with structural element lesions. The four sites proximal to *8* have been carefully aligned, and the complementing mutant *606* is the most proximal of these. No null mutant appears to be proximal to *606*. Among the non-complementers, *23* appears to be the most proximal. Present data indicate that both *606* and *23* mark the proximal boundary of the XDH structural element.

Thus far, the distal portion of the structural element has been treated more casually. Nonetheless, we now have five structural sites distal to *8*. These include two electrophoretic sites which were previously identified (*e508* and *e111*) and three null mutants (*2*, *42*, and *501*) which later turned out to be complementing alleles. If we pursued the localization of *207*, *609*, *ps611*, *ps612* and *L.19*, presumably more structural sites distal to *8* would be resolved. The most distal of the previously mapped sites are *e111* and *2*. We infer that *e111* must be distal to *41* by the following logic, derived from earlier data (GELBART *et al.* 1974). Co-conversions of *e111* and *41* occur at a rate of only 30%. If *e111* were proximal to *41*, recombination tests of *41* with more proximal *100* alleles (*102*, *103*, *106* and *110*) should generate some crossovers between *e111* and *41*. However, none were recovered among sixty crossovers. CHOVNICK, BALLANTYNE and HOLM (1971)

demonstrated that *2* is also distal to *41*. Because of the "prehistoric" origin of *2*, a spontaneous mutant whose pedigree is unknown, it would be experimentally difficult to ever align *2* and *e111*. Regardless of the order of these two sites, they represent both the most distal rosy mutants and the distal limit of the XDH structural element as well.

Every rosy eye color mutant (null-XDH) is now included within the structural element. We have no null mutant sites, either radiation- or EMS-induced, which fall outside of this region, and which might be candidates for control element alterations. The structural element now includes the entire 0.005 map unit segment identified as the rosy locus. Since this length has been revised from our earlier estimates (See MATERIALS AND METHODS), it behooves us to reexamine the relationship between genetic and physical estimates of the length of DNA comprising the structural element. We can make two independent estimates of this length.

(1) We can directly compute the size of this DNA tract from the size of the XDH polypeptide subunit. This subunit molecular weight has been estimated at 160,000 daltons (CANDIDO and BAILLIE, unpublished), and therefore, should be coded by a DNA segment approximately 3 kilobases (kB) in length.

(2) An indirect estimate of the length of DNA in the XDH structural element can be derived from its genetic length of 0.005 map units. To do so, we must have a constant which relates map distance to DNA length. We can simply divide the total euchromatic DNA in the haploid genome by the map length of the genome (1.6×10^5 kB/ 275 map units = 5.8 kB/ 0.01 map unit). (The 1.6×10^5 kB estimate is that proportion of the total genome DNA represented as single-copy and middle repetitive sequences (.88—MANNING, SCHMID and DAVIDSON 1975) multiplied by the total genome size [RASCH, BARR and RASCH 1971].) Using this constant, the XDH structural element would measure 2.9 kB, strikingly close to the direct physical estimate!

LEFEVRE (1971) calculated that 0.01 map units equates with 3.7 to 3.8 kB of DNA (compared to our estimate of 5.8 kB). The reader should recognize that our estimate cancels out regional differences in crossover frequency and in addition eliminates the impact of highly repetitive DNA (centromeric heterochromatin) which exhibits little, if any, recombination. However, LEFEVRE's estimate emerges from a comparison of crossover frequency and DNA content in a region of the genome exhibiting a relatively high rate of recombination. In fact, rosy is located in a region exhibiting a somewhat reduced rate of exchange due to the "centromere effect" (BEADLE 1932; THOMPSON 1964). This statement emerges from a consideration of the cytogenetics of the right arm of chromosome *3*. It contains 1178 polytene bands (BRIDGES 1941) and is approximately 55 map units in length (LINDSLEY and GRELL 1968). The rosy locus (87D8-12) is located approximately 1/3 of the distance from the chromocentral end of 3R to the distal tip (368/1178 bands). However, in terms of recombination frequency, it is less than 1/10 of this distance (4/55 map units). Clearly, recombination in the rosy region is reduced relative to more distal chromosome segments.

New categories of rosy mutants:

In this report, we have described phenotypic complementation among rosy eye color mutants. These complementing mutants represent a new class of XDH structural variants. We have noted a correlation between map position and complementation pattern: mutants proximal to *8* complement only with some of the mutants distal to *8*, and vice versa. No proximal-proximal or distal-distal completing pairs have been noted. Presumably, this is a reflection of the three dimensional structure of XDH; if this relationship holds, it could serve as an indicator of map position of new complementing alleles.

We have also described a protocol for the selection of purine-sensitive mutants and presented results of our initial screen. Because of the general subject of this report, we focused upon three purine-sensitive rosy alleles which were unambiguous structural variants. Note that this selection scheme may also permit recovery of control element lesions.

The importance of delimiting the structural element:

In summary, a number of new structural sites have been identified within the rosy locus. Of these, a complementing mutant, ry^{606}, represents our present proximal limit to the XDH structural element, and ry^{2} or ry^{e111} represent our distal limit. The establishment of these limits will provide an important assay for XDH control variants. Such variants should map either proximal to ry^{606} or distal to ry^{2} and ry^{e111}. The companion paper (CHOVNICK *et al.* 1976) describes one such variant, confirming the utility of this approach.

We gratefully acknowledge the excellent technical assistance of HAROLD LEVINE, FLORENCE JOHNSTON, ARTHUR KING and PHIL COLLIS.

LITERATURE CITED

BEADLE, G., 1932 A possible influence of the spindle fiber on crossing-over in Drosophila. Proc. Natl. Acad. Sci. U.S. **18:** 160–165.

BRIDGES, P. N., 1941 A revision of the salivary gland 3R-chromosome map of *Drosophila melanogaster*. J. Hered. **32:** 299–300.

CANDIDO, E., D. BAILLIE and A. CHOVNICK, 1974 A rapid purification of xanthine dehydrogenase for genetic studies. Genetics **77:** 59 (Abstr.).

CHOVNICK, A., 1973 Gene conversion and transfer of genetic information within the inverted region of inversion heterozygotes. Genetics **75:** 123–131.

CHOVNICK, A., G. BALLANTYNE, D. BAILLIE and D. HOLM, 1970 Gene conversion in higher organisms: half-tetrad analysis of recombination within the rosy cistron of *Drosophila melanogaster*. Genetics **66:** 315–329.

CHOVNICK, A., G. BALLANTYNE and D. HOLM, 1971 Studies on gene conversion and its relationship to linked exchange in *Drosophila melanogaster*. Genetics **69:** 179–209.

CHOVNICK, A., W. GELBART, M. MCCARRON, B. OSMOND, P. CANDIDO and D. BAILLIE, 1976 Organization of the rosy locus in *Drosophila melanogaster*: Evidence for a control element adjacent to the xanthine dehydrogenase structural element. Genetics **84:** ...–....

CHOVNICK, A., A. SCHALET, R. KERNAGHAN and M. KRAUSS, 1964 The rosy cistron in *Drosophila melanogaster*: Genetic fine structure analysis. Genetics **50:** 1245–1259.

CRICK, F. and L. ORGEL, 1964 The theory of inter-allelic complementation. J. Mol. Biol. **8:** 161–165.

FINCHAM, J., 1966 *Genetic Complementation.* W. A. Benjamin, New York.

GELBART, W., M. MCCARRON, J. PANDEY and A. CHOVNICK, 1974 Genetic limits of the xanthine dehydrogenase structural element within the rosy locus in *Drosophila melanogaster.* Genetics **78:** 869–886.

HOCHMAN, B., 1973 Analysis of a whole chromosome in Drosophila. Cold Spring Harbor Symp. Quant. Biol: **38:** 581–589.

JUDD, B., M. SHEN and T. KAUFMAN, 1972 The anatomy and function of a segment of the *X* chromosome of *Drosophila melanogaster.* Genetics **71:** 139–156.

LAIRD, C., 1973 DNA of Drosophila chromosomes. Ann. Rev. Genet. **7:** 177–204.

LAURELL, C., 1966 Quantitative estimation of proteins by electophoresis in agarose gel containing antibodies. Anal. Biochem. **15:** 45–52.

LEFEVRE, G., 1971 Salivary chromosome bands and the frequency of crossing over in *Drosophila melanogaster.* Genetics **67:** 497–513. ——, 1973 The one band—one gene hypothesis: Evidence from a cytogenetic analysis of mutant and nonmutant rearrangement breakpoints in *Drosophila melanogaster.* Cold Spring Harbor Symp. Quant. Biol. **38:** 591–599.

LEVY, B. and B. MCCARTHY, 1975 Messenger RNA complexity in *Drosophila melanogaster.* Biochemistry **14:** 2440–2446.

LEWIS, E. and F. BACHER, 1968 Method for feeding ethyl methane sulfonate (EMS) to Drosophila males. Drosophila Inform. Serv. **43:** 193.

LINDSLEY, D. and E. GRELL, 1968 Genetic variations of *Drosophila melanogaster.* Publ. Carnegie Inst. Washington No. 627.

MANNING, J., C. SCHMID and N. DAVIDSON, 1975 Interspersion of repetitive and nonrepetitive DNA sequences in the *Drosophila melanogaster* genome. Cell **4:** 141–155.

MCCARRON, M., W. GELBART and A. CHOVNICK, 1974 Intracistronic mapping of electrophoretic sites in *Drosophila melanogaster*: Fidelity of information transfer by gene conversion. Genetics **76:** 289–299.

RASCH, E., H. BARR and R. RASCH, 1971 The DNA content of sperm of *Drosophila melanogaster.* Chromosoma **33:** 1–18.

SCHALET, A., R. KERNAGHAN and A. CHOVNICK, 1964. Structural and phenotypic definition of the rosy cistron in *Drosophila melanogaster.* Genetics **50:** 1261–1268.

THOMPSON, P., 1964 Evidence on the basis of the centromere effect in the large autosomes of *Drosophila melanogaster.* Genetics **49:** 761–769.

YEN, T. and E. GLASSMAN, 1965 Electrophoretic variants of xanthine dehydrogenase in *Drosophila melanogaster.* Genetics **52:** 977–981.

Corresponding editor: D. R. STADLER